Global Scientific JOURNALS

GSJ: Volume 7, Issue 5, May 2019, Online: ISSN 2320-9186
www.globalscientificjournal.com

MASSIVE MIMO FOR HIGH-SPEED TRAIN COMMUNICATION SYSTEMS

[1*] Majin Rachael Nnagana, [2] Adewara D. Olanrewaju, [3]Jiya Zachariah, [4]Olanite Olanrewaju Ade, [5]Adamu Yunusa
[1*,2,3]Department of Electrical and Electronic Engineering, Niger State Polytechnic, Zungeru, Nigeria.
Correspondence Email/GSM: samshidali@gmail.com/+2348060989804

ABSTRACT

With the current development in wireless communications in high-mobility systems such as high-speed train (HST), the HST scenario is recognised as one of the scenarios for the fifth generation (5G). Massive Multiple-Input-Multiple-Output (MIMO) systems, which are equipped with tens or hundreds of antennas has become an enhanced MIMO technique which can help in meeting the increasing demand of data for 5G wireless communication systems. In this study, the related 5G technologies and the corresponding channel modelling in HST scenarios and the challenges of deploying massive MIMO on HST was investigated The channel model was modelled using the WINNER II channel model. Based on the proposed non-stationary IMT-A massive MIMO channel models, the essential statistical properties such as the spatial cross-correlation function (CCF), local temporal autocorrelation function (ACF) of the massive MIMO channel model using different propagation scenarios such as open space, viaduct and cutting was analysed and investigated. The results from the simulations was compared with the analytical results in other to show that the statistical properties vary with time as a result of the non-stationarity of the proposed channel model. The agreement between the stationary interval of the non-stationary IMT-A channel model and the HST under different propagation scenarios shows the efficiency of the proposed channel model. Based on findings; the impact of the deployment of large antenna on the channel capacity should be thoroughly investigated under different HST propagation scenario. Also, more HST train propagation scenarios such as the tunnel, hilly terrain and the station should be considered in the non-stationary IMT-A massive MIMO channel models.

1.0 Introduction

The focus of mobile communication research, development and operation has since been on spectrum efficiency, the spatial multiplexing discovery through the use of multiple antennas in the mid-1990s brought new achievement to data rate boosting despite the limited bandwidth. Recently, it has become standard to equip the Base Stations (BSs) with an antenna array that

aid various functionalities of the Massive Multiple-Input-Multiple-Output (MIMO) systems MIMO which includes; the multiplexing, diversity, beam forming, and interference coordination (Xiang Cheng *et al.*, 2014).

The MIMO recently draws much attention as a promising technique which can enhance the performance, link reliability and capacity, link rates, enhance the network throughput of the communication system, which is also to mainly increase the spectral efficiency of the communication system (Ghazal, 2017; Xie *et al.,* 2015).

In the evaluation and designing of MIMO wireless communication system, channel modelling performs an essential role, the demonstration of the feasibility of the wireless system cannot be realised without the accurate channel model that can mimic the important characteristics of the wireless channels (Ghazal, 2017).

MIMO is deployed in a lot of advanced wireless communication system such as the Long-term evolution (LTE), Worldwide Interoperability for the microwave access (WiMAX) etc. (Wu *et al.,* 2015). There are many standardised MIMO channel model such as the long term evolution-advanced (LTE-A), 3rd generation partnership project (3GPPP/3GPP2) spatial channel model (SCM), SCM-Extension (SCME), WINNER I, WINNER II, WINNER + and IMT-A channel models (Ghazal, 2017; Wu *et al.,* 2015); but most of this mention channel models cannot sufficiently be able to capture specific characteristics of massive MIMO (Wu *et al.,* 2015), they neglect the non-stationarity of the fading channels which assumes that the channel satisfies the wide sense stationary (WSS) (Ghazal, 2017).

The recent introduction of massive MIMO systems which are equipped with tens or hundreds of antennas is mostly and broadly recognised as one of the most important technologies which emerged as an improved MIMO technique to the increasing traffic demand for the 5G wireless communications (Wu *et al.,* 2014; Bai *et al.,* 2017). The massive MIMO system has more benefits than the conventional MIMO systems with less number of antennas, the performances of the system regarding capacity, reliability and energy efficiency and spectral efficiency is considerably better than the conventional MIMO systems (Wu *et al.,* 2014; Zhang *et al.,* 2017).

The massive MIMO channel system is not only equipped with tens or even hundreds of antennas, but it has a peculiar channel characteristics that include the non-stationary channel characteristics in time and array domain, spherical wavefront propagation which is modelled in the massive MIMO channel model in decreasing the correlation of the Channel Impulse

Responses (CIRs) thereby increasing the capacity of the channel (Xie *et al.,* 2015; Bai *et al.,* 2017).

The large scale and the small scale fading which has a significant impact on the system performance of the 5G wireless system will be looked into (Wu *et al.,* 2014; Wu *et al.,* 2017).

HST communication system also draws the attention for the emerging advancement for high mobility trains with an expected speed of over 500km/hr (Wu *et al.,* 2017). The high-speed mobile wireless communication systems encounter the challenge of providing constant communication services over fast-changing radio channel unfavourable environmental scenarios such as a tunnel, viaduct, subway and so on (Ghazal, 2017).

Due to the high mobility and non-stationarity of HST, massive MIMO will be deployed on the HST to enhance the data throughput, spatial efficiency of the channel will be modelled under different HST propagation scenarios. IMT-A and WINNER II channel model which uses the geometry-based stochastic models (GBSMs) channel model will be used to model the HST channels under different propagation scenarios where the detailed descriptions of the propagation for the environments and the computational resources will be required (Ghazal, 2017).

Based on the non - stationary IMT-A massive MIMO channel model, the statistical properties such as the spatial CCF, autocorrelation function (ACF) will be investigated and analysed, and the stationary interval of the proposed channel model will also be investigated (Ghazal, 2017). The results gotten from simulation will be compared with the analytical results in other to demonstrate the efficiency of the proposed channel model.

It is against this background that this study attempts to investigate the deployment of massive MIMO technique on HST under different propagation scenarios such as; the open space, viaduct and the cutting. Also to investigate the related 5G important technologies and the corresponding channel modelling in HST scenarios that lead to increasing demand for data of the 5G wireless communications.

2.0 Literature Review

The prediction for the mobile traffic is to grow more than 1000 times in the next 10 years, which the International Mobile Telecommunication (IMT) alongside with vision 2020 and

beyond desires a future 5G wireless communication systems to be able to deliver a peak data rate of 10Gps, this leads to emergence of the massive MIMO technology (Jianhua, 2017).

The use of multi-users MIMO gives huge advantages over the conventional point-to-point MIMO, the multi-user works with inexpensive single-antenna terminals which do not require rich scattering environment, and the allocation of resource is simplified because every active terminal utilises all of the time-frequency bins (Larsson *et al.,* 2014). Although multi-user MIMO originally anticipated that the use of roughly equal numbers of service antenna, terminal and frequency-division duplex (FDD) is not an adaptable technology (Larsson *et al.,* 2014).

Massive MIMO system has a large number of the antenna which is typically tens or hundreds that serves many tens of terminals that have the same time-frequency resource. It provides better performance in spectrum efficiency, reliability, robust and channel capacity; it is also used as an enabler for infrastructure for the future digital society that will connect the internet of things and internet of people with the clouds and also with other network infrastructures (Jianhua, 2017; Larsson *et al.*, 2014).

Series of measurement campaign of massive MIMO has been carried out to evaluate the performance of the channel, for example, the outdoor channel measurement with a linear virtual array and cylindrical array of 128 antennas elements and carrier frequency of 2.6GHz which studied the capacity, sum rate, precoding schemes and spectrum efficiency, and also an outdoor static measurement campaign in a stadium was performed and analysed with the use of a linear 128 antenna element virtual array with frequency of 1.4725GHz and an angular power spectrum was used in the massive MIMO measurement (Jianhua, 2017).

2.1 High-Speed Train (HST)

High-Speed Train, also called High-Speed Railway is known for bringing comfort to the lives of people, it is famous as the most viable developments for ground transportation, the signalling system which is also called the operation control system is one of the important parts of the HST construction where the wireless communication performs an important role in the transmission of data for the train control (Ai, 2014). The growth of HST in the world has made the maximum moving speed of the train to reach nearly 575km/h, the issue of safety in the train operation has drawn more attention due to the increase in the train speed (Ai, 2014). The three main part contributing to the safe operation of the HST is namely: the ground infrastructure

(e.g. trackside equipment), the moving body (e.g. the train), and the signalling system. Out of the three main parts, the signalling system which is also called the operation control system of the train is an important part of the train which is regarded as the HST system nerve centre (Ai, 2014).

Global system for mobile communications for railway (GSM-R) which is a narrow-band communication system performs an important role in the safe operation of the HST to make the operation of the train control system to work better and also to maintain a reliable link in communication between the train and the ground (Ai, 2014). In Ai (2014), the long-term evolution of railway (LTE-R) which is a broadband communication system was also deployed due to the fast growth in the railway service.

HST scenario which is one of the high-mobility scenarios is expected to be one of the typical 5G communication systems, due to the fast development in the HST, increasing the capacity of wireless communication data is needed to be transferred to the passengers on the train (Wang *et al.,* 2016). The HST users requires sufficient network with reliable communication services regardless of their location and the speed of the train, in order to satisfy this requirement, HST wireless communication system has to overcome several challenges due to the effect of the high speed of the train that can easily exceed 250km/h; some of the challenges are; fast travel through different scenarios, doppler spread, fast handover and also some challenges inherited from conventional trains such as; limited visibility in tunnels, harsh electromagnetic environment and high penetration losses (Wang *et al.,* 2016; Ghazal *et al.,* 2016).

In Ai (2014), it was stated that whether the system of communication in the HST is GSM-R, an LTE-R or an IEEE 802. 15.4p, to get a reliable communication, the most important condition is to have the full knowledge of the propagation characteristics of the wireless channel; wireless channel modelling is an essential basis and a vital means for planning and optimization for communication network, the design of the transmitter and receiver and also the physical and upper layer in choosing the important technologies (Ai, 2014).

Many research studies on wireless channel measurement and modelling were performed; for example Rappaport *et al*. worked on 60GHz wireless communications and channel modelling, Matolak *et al*. studied on vehicle-to vehicle (V2V) channel modelling, Sivertsen *et al*., Cheng *et al*. and Guan *et al*. researched on the multi input-multi-output orthogonal frequency-division multiplexing (MIMO-OFDM) channel modelling, ray-tracing technique and geometry-based stochastic channel modelling (GBSM); lots of works on channel modelling, supply of channel

measurement instruments and standardization were done by project groups such as COST, WINNER and MEDAV (Ai, 2014).

2.1.1 Classification of different scenarios in HST

The transmitter and receiver for the HST wireless communication system are faced with different challenges in the channel condition because the train has to pass through various scenarios and geographical environment. The different environment can be classified into six (6) scenarios such as; open space, cutting, viaduct, tunnel, hilly terrain and stations (Wang *et al.*, 2016; Ghazal *et al.*, 2016); Figure 1 shows further classification of the HST scenarios.

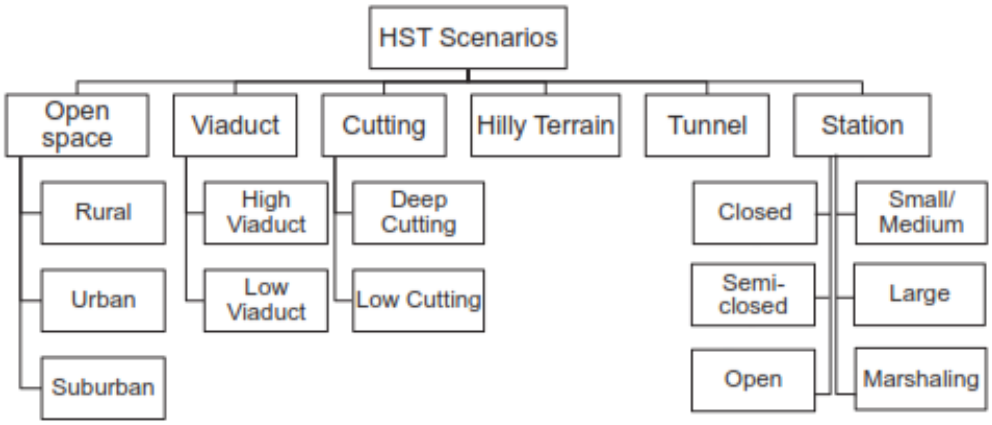

Figure 1: The classification of HST scenarios

2.2 Massive MIMO

Massive MIMO which is also known as large-scale antenna system, hyper MIMO, very large MIMO, ARGOS and full dimension MIMO is an emerging technology where tens and hundreds of antennas give greater performance in reliability, capacity, efficiency. Massive MIMO is also robust against unintended man-made interference; it can improve the channel capacity, reduce latency on the air interface and international jamming (Jianhua, 2017; Larsson, 2014), (Gao *et al.*, 2013; Wang *et al.*, 2016). Massive MIMO considers the multi-user MIMO (MU-MIMO) where the BS is equipped with arrays of antennas (tens and hundreds of antennas) that is serving many tens of terminals in the same time-frequency resources (Larsson, 2014; (Gao *et al.*, 2013; Wang *et al.*, 2016).

Massive MIMO is an enhanced MIMO technique that is used to meet the increasing traffic demand of the 5G wireless communication network; massive MIMO has some benefits as compared to conventional MIMO such as;

- Sufficiently increasing the energy efficiency as power is concentrated in a sharp direction.
- Boosting of the system throughput by the utilisation of MU-MIMO, the introduction of a huge number of antennas according to the large number theorem reduces the interference between users.
- Reduction in the cost of implementation by including the simplification of medium-access control layer and by the use of low-cost antenna elements as a result of very large MU-MIMO and beamforming gain.
- Massive MIMO offers more degree of freedom because it is more robust than the conventional MIMO systems (Wu *et al.,* 2014; Larsson, 2014; Wang *et al.,* 2016).

Massive MIMO depends on spatial multiplexing which in turns depends on the BS to have better knowledge of the channel on both uplink and downlink. In the uplink, it is easy to accomplish because the terminals send pilots based on which the BS estimates the response of the channel response to every terminal, but in downlink, it is more difficult (Larsson, 2014).

Massive MIMO is used to enable the development of the future broadband networks that are energy efficient, robust, secure and that will use the spectrum efficiency. It is also an enabler for the digital society infrastructure in the future that will connect the internet of things and internet of people with clouds and other infrastructures (Larsson, 2014).

Both theory and real propagation environments have shown that massive MIMO systems have very promising properties due to its many benefits such as energy efficiency, highly improving the spectral efficiency and robustness of the system as compared to the conventional MIMO systems that have a small number of antennas at the BS (Gao *et al.,* 2013; Wang *et al.,* 2016). To efficiently evaluate the new technique in massive MIMO in more practical scenarios, new channel models are required to capture the essential properties of the real massive MIMO propagation channels. Massive MIMO can have antenna arrays that span tens or hundreds of wavelength in space due to its large number of antennas (Gao *et al.,* 2013).

The novelty of this research is the deploying of massive MIMO on HST and using the WINNER II channel model in modelling the channel. Based on the non-stationary IMT-A

massive MIMO channel model, the statistical properties such as; spatial CCF and local temporal ACF will be derived and analysed under different HST propagation scenarios such as; the open space, viaduct and cutting. The stationary interval of the proposed channel model will be investigated and will be compared with the original non-stationary IMT-A MIMO channel model in other to demonstrate the efficiency of the proposed channel model.

3.0 Methodology

In this study, massive MIMO technique was deployed on HST under different scenarios; the radio channel was modelled under the HST wireless communication system with different propagation scenarios such as the open space, viaduct and cutting. The massive MIMO characteristics such as the non-stationarity and the spherical wavefront of the channel was captured and investigated.

The GBSMs channel model was used in modelling of the massive MIMO on HST channel model. GBSMs is one of the recent advances in conventional MIMO systems, although the channel model can model the MIMO channels more accurately taking into consideration the key characteristics of the channel, it has higher computational complexity (Wang *et al.*, 2016).

The non-stationarity properties of the clusters such as the appearance and disappearance on the time axes and the array was modelled by the use of birth-death process and the impact of the spherical wavefront on the Doppler frequencies on the antenna array as a results of increased number of antennas was captured (Gao *et al.*, 2013; Wang *et al.*, 2016).

The IMT-A system using the WINNER II channel model was adopted on the HST wireless communication system under the open space, viaduct and the cutting scenarios. Key statistical properties such as the local spatial CCF, local temporal ACF was derived and analysed, the correlation and the effect on the channel capacity for the different scenarios was compared, and non-stationarity interval of the channel model was also investigated (Ghazal, 2017).

The mobile relay technology that was adopted by the IMT-A system and the WINNER II channel model was used in the deployment of the massive MIMO system on the HST, dedicated MRS was deployed on the top of the train in other to extend the coverage at the outdoor BS into the carriages of the train, this leads to having two channels which are; an outdoor channel between the BS and the MRS, and an indoor channel between the MRS and the MS which is illustrated in Figure 2 (Wang *et al.*, 2016; Ghazal, 2015).

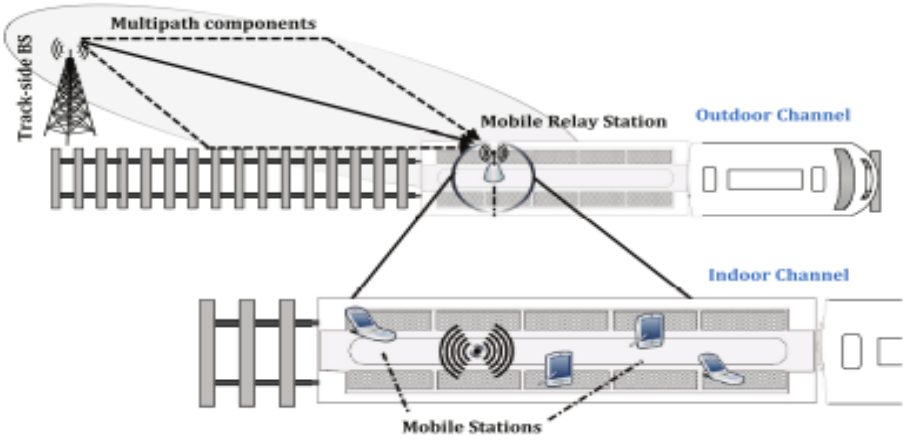

Figure 2: Deployment of MRSs on HST communication system

From Figure 2, the BS mainly communicate with the MRS at high data rate rather than directly communicating with large numbers of MRSs, the MRSs together with the MSs inside the train carriage are all seen as one unit to the BS while MRSs views the relevant MRSs as a normal BS. The repeated handover problem on HST systems can greatly be reduced by the MRS performing a group of handover on behalf of the associated MSs (Wang *et al.*, 2016).

In the IMT-A systems where the generic model which is based on WINNER II channel model gives the detailed mathematical model and the algorithms that are used for the channel modelling in all scenarios, the model makes use of the GBSM approach in representing the multipath propagation channel between BSs to the MSs (Ghazal, 2017). The channel in IMT-A channel model is assumed to satisfy the WSSUS assumption which means that the statistics of the channel fading remains invariant in the time domain over a short period where the scatterers with different path delays are uncorrelated, based on the assumption of the WSSUS and the concept of the tap delay line (TDL), the complex CIR between antenna element s(s = 1, …, S) of the BS and the antenna elements u(u = 1, …, U) of the MS of the IMT-A MIMO channel model is given as (Ghazal, 2017);

$$h_{u,s}(t,\tau) = \sum_{n=1}^{N} h_{u,s,n}(t)\delta(\tau - \tau_n) \qquad (1)$$

Where,

$$h_{u,s,n}(t) = \sqrt{\frac{P_n}{M}} \sum_{m=1}^{M} e^{jd_s k \sin(\phi_{n,m})} e^{jd_u k \sin(\varphi_{n,m})} \times e^{j2\pi v_{n,m} t} e^{j\Phi_{n,m}}. \qquad (2)$$

In this equation $h_{u,s,n}(t)$ $(n = 1, \dots, N)$ denotes a narrow process where all the M sub-paths in every N clusters are irresolvable rays that have the same delay τ_n, the power of the nth cluster associated with the delay τ_n, is given as P_n, the antenna element spacing at the BS and the MS is given as d_s and d_u respectively, the wave number is $k = \frac{2\pi}{\lambda}$ where λ is the carrier wavelength, the AoD and AoA related to the $mth(m = 1, \dots, M)$ ray within the $nth(n = 1, \dots, N)$ cluster is given as $\phi_{n,m}$ and $\varphi_{n,m}$ respectively and the random phases $\Phi_{n,m}$ are distributed uniformly within [- π, π]. The Doppler frequency component is given by $\frac{||\bar{v}MS||\cos(\varphi_{n,m} - \theta_{MS})}{\lambda}$ where $||\vec{v}_{MS}||$ and θ_{MS} represents the magnitude of the MS velocity and direction of travel for the MS respectively, all of the parameters mentioned above are time-invariant because of the WSSUS assumption of the IMT-A channel model (Ghazal, 2017).

3.1 The non-stationary IMT-A channel model with the time-varying parameters

Due to the noticeable movement of the MC and MSs, the assumption for WSSUS will be violated while the channel parameters changes with time, the CIR of the non-stationary IMT-A channel model with time-varying parameters, in this case, can be expressed as;

$$h_{u,s}(t, \tau) = \sum_{n=1}^{N(t)} h_{u,s,n}(t)\, \delta(\tau - \tau_n(t)) \tag{3}$$

where

$$h_{u,s,n}(t) = \sqrt{\frac{P_n(t)}{M}} \sum_{m=1}^{M} e^{jd_s k \sin(\phi_{n,m}(t))} e^{jd_u k \sin(\varphi_{n,m}(t))} \times e^{jk||\vec{v}_{MS}||\cos(\varphi_{n,m}(t) - \theta_{MS})t} e^{j\Phi_{n,m}}. \tag{4}$$

As a result of the movement of the MC and the MSs, the parameters of the channel $N(t)$, τ_n, $P_n(t)$, $\phi_{n,m}(t)$, and $\varphi_{n,m}(t)$ changes with time and hence, requires to be represented using proper time-varying functions, the IMT-A channel model is illustrated in Figure 3 (Ghazal, 2017).

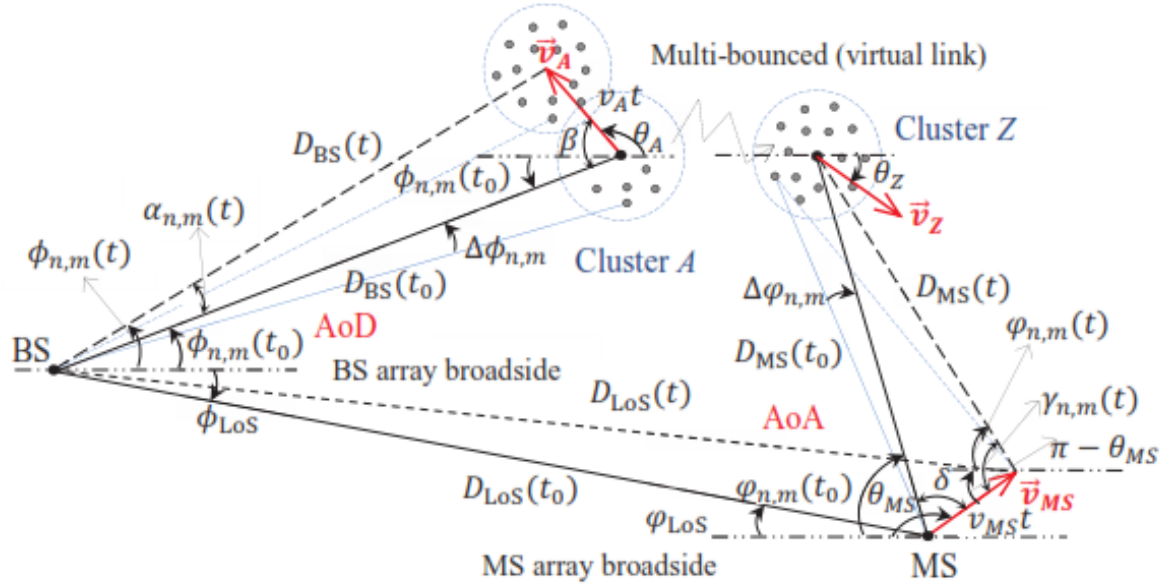

Figure 3: Angular parameters for BS and MS in the IMT-A channel model

In this channel, the propagation between the first and the last related cluster is not defined, although multiple interactions with scattering media can also be model in the same way. Note that the initial AoD, initial AoA, AoD offset and AoA offset is given as $\phi_{n,m}(t_o)$, $\varphi_{n,m}(t_o)$, $\Delta\phi_{n,m}(t_o)$, $\Delta\varphi_{n,m}(t_o)$ respectively, one of the *N* path and one of the *M* ray/sub-paths in the wideband channel model is indicated by the subscripts n, m respectively (Ghazal, 2017).

The first bounce/cluster (i.e. cluster *A*) describes the AoD which is interacted from the BS side and the last bounce/cluster (i.e. cluster *Z*) describes the AoA, in addition, the LoS components for the BS and MS are denoted by ϕLoS, and φLoS respectively, from Figure 3 it is assumed that the BS is fixed and the first cluster, Cluster *A* is moving with the direction θ_A and with the speed of v_A (Ghazal, 2017). The multi-bounced scattering which takes place from each path is been considered as the last bounce MC and is referred to as Cluster *Z* with the moving direction θ_Z and the speed v_Z, for the MS, the moving direction is given as θ_{MS} and speed v_{MS}, the vectors $\vec{v}_A$, $\vec{v}_Z$ and $\vec{v}_{MS}$ represents the movement of MC *A*, MC *Z* and MS in Figure 3. The initial distance between the BS and MC *A* and the initial distance between the MS and MC *Z* which are given as $D_{BS}(t_o)$ and $D_{MS}(t_o)$ are assumed to be known, and the initial distance of the LoS components between the BS and the MS is given as $D_{LoS}(t_o)$ (Ghazal, 2017).

Four assistant angles are sets in Figure 3 in other to derive the time-varying angular parameters, they are; $\alpha_{n,m}(t)$, β, $\gamma_{n,m}(t)$ and δ, note that only LoS path and the nth scattered propagation path are presented in the Figure 3. For example, Cluster *A* corresponds to the first bounce while

Cluster Z corresponds to the last bounce of the nth scattered path, if MC A and MC Z is static, the speed v_A of the MC A and speed v_Z of MC Z can be set to zero and this will not affect the generation procedure of the channel coefficients in the non-stationary IMT-A MIMO channel model (Ghazal, 2017).

Based on the geometric description of the channel above, Figure 4 illustrates the procedure to obtain the channel realisation of the non-stationary IMT-A channel model where the initial values of the channel model parameters such as $\tau_n(t_o)$, $P_n(t_o)$, $\phi_{n,m}(t_o)$, and $\varphi_{n,m}(t_o)$, are calculated using the same procedure presented in the original IMT-A channel model (i.e. at the top section of Figure 4) (Ghazal, 2017).

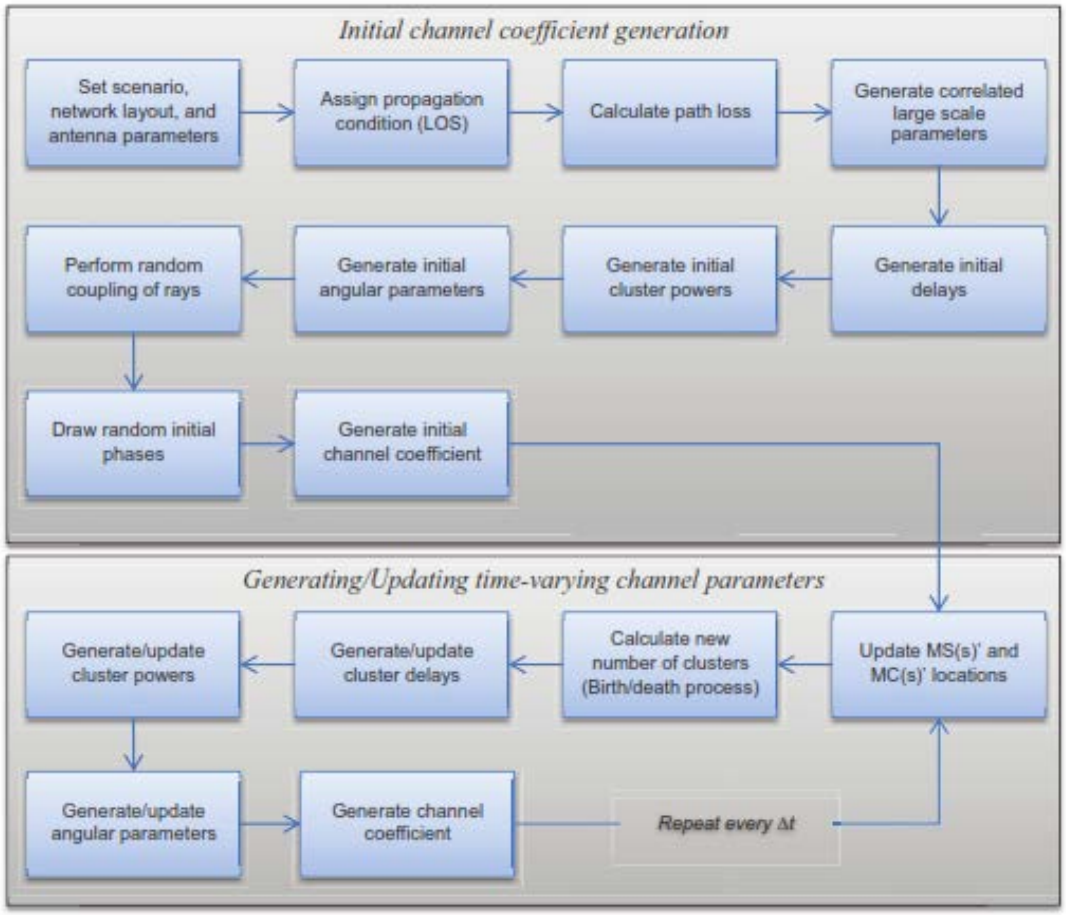

Figure 4: Generation procedure for the non-stationary IMT-A channel coefficients

The focus here will be on the non-stationarity properties of the IMT-A channel model (which is at the bottom section of Figure 3) (Ghazal, 2017).

3.2 The stationary interval of the channel model

The average power delay profiles (APDPs) is used in calculating the stationary interval of the channel model, and it is given as;

$$\overline{P_h}(t_k, \tau) = \frac{1}{N_{PDP}} \sum_{k}^{k+N_{PDP}-1} |h_{u,s}(t_k, \tau)|^2 \quad (35)$$

Where N_{PDP} denotes the number of power delay profiles to be averaged, *tk* is the time of the *kth* drop and $h_{u,s}(t_k, \tau) = \sum_{n=1}^{N} h_{u,s,n}(t_k)\,\delta(\tau - \tau_n)$.

The correlation coefficient between two APDPs can be calculated as [2]

$$c(t_k, \Delta t) = \frac{\int \overline{P_h}(t_k, \tau)\,\overline{P_h}(t_k + \Delta t, \tau)\,\mathrm{d}\tau}{\max\{\int \overline{P_h}(t_k, \tau)^2\,\mathrm{d}\tau, \int \overline{P_h}(t_k + \Delta t, \tau)^2\,\mathrm{d}\tau\}}. \quad (36)$$

Therefore, the stationary interval can be calculated as

$$T_s(t_k) = \max\{\Delta t|_{c(t_k, \Delta t) \geq c_{\text{thresh}}}\} \quad (37)$$

Where the threshold of the correlation coefficient is given as c_{thresh} (Ghazal, 2017).

The documentation for the source code for MATLAB implementation for WINNER II channel model from reference was used for writing the MATLAB programs that was used to perform the simulation for the channel model. The channel model parameters for the scenarios were set up in accordance the ITU-R M.2135-1 (Report ITU-R M.2135-1, 2009).

Table A1-7 in the ITU-R M.2135-1 (Report ITU-R M.2135-1, 2009) was used for the channel parameter setup; the table was upgraded by the addition of viaduct and the cutting scenarios.

From the table A1-7 in the ITU-R M.2135-1 (Report ITU-R M.2135-1, 2009), the following are represented as;
DS: rms delay spread, ASD: rms azimuth spread of departure angles, ASA: rms azimuth spread of arrival angle, SF: shadow fading and K: Ricean *K*-factor. The sign for the shadow fading is defined such that the positive SF means more received power at the UT than predicted by the path loss model (Report ITU-R M.2135-1, 2009).

The DS, SF and the K-factor for the new scenarios were obtained from channel measurements on HST; the channel measurements were obtained from references (Guo *et al.,* 2013) for the viaduct, (Tian *et al.,* 2013 and Sun *et al.,* 2013) for the cutting scenario.

Table 1: Channel model parameters setup

SCENARIOS		**RMa (Open Space)**		**Viaduct**		**Cutting**	
		LoS	**NLoS**	**LoS**	**NLoS**	**LoS**	**NLoS**
Delay spread (DS) $\log_{10}$(s)	μ	-7.49	-7.43	-7.04	-7.43	-6.71	-7.43
	σ	0.55	0.48	0.54	0.48	0.40	0.48
AoD spread (ASD) $\log_{10}$(degrees)	μ	0.90	0.95	0.90	0.95	0.90	0.95
	σ	0.38	0.45	0.38	0.45	0.38	0.45
AoA spread (ASA) $\log_{10}$(degrees)	μ	1.52	1.52	1.52	1.52	1.52	1.52
	σ	0.24	0.13	0.24	0.13	0.24	0.13
Shadow fading (SF) (dB)	σ	4	8	4.8	8	1.66	8
K-factor (*K*) (dB)	μ	7	N/A	8.78	N/A	0	N/A
	σ	4	N/A	6.08	N/A	3.23	N/A
Cross-correlation*	ASD vs DS	0	-0.4	0	-0.4	0	-0.4
	ASA vs DS	0	0	0	0	0	0
	ASA vs SF	0	0	0	0	0	0
	ASD vs SF	0	0.6	0	0.6	0	0.6
	DS vs SF	-0.5	-0.5	-0.5	-0.5	-0.5	-0.5
	ASD vs ASA	0	0	0	0	0	0
	ASD vs *K*	0	N/A	0	N/A	0	N/A
	ASA vs *K*	0	N/A	0	N/A	0	N/A
	DS vs *K*	0	N/A	0	N/A	0	N/A
	SF vs *K*	0	N/A	0	N/A	0	N/A
Delay distribution		Exp	Exp	Exp	Exp	Exp	Exp
AoD and AoA distribution		Wrapped Gaussian		N/A		N/A	
Delay scaling parameter r_τ		3.8	1.7	3.8	1.7	3.8	1.7
XPR (dB)	μ	12	7	12	7	12	7

Number of clusters		11	10	11	10	11	10
Number of rays per cluster		20	20	20	20	20	20
Cluster ASD		2	2	2	2	2	2
Cluster ASA		3	3	3	3	3	3
Per cluster shadowing std ζ (dB)		3	3	3	3	3	3
Correlation distance (m)	DS	50	36	50	36	50	36
	ASD	25	30	25	30	25	30
	ASA	35	40	35	40	35	40
	SF	37	120	37	120	37	120
	K	40	N/A	40	N/A	40	N/A

4.0 RESULTS

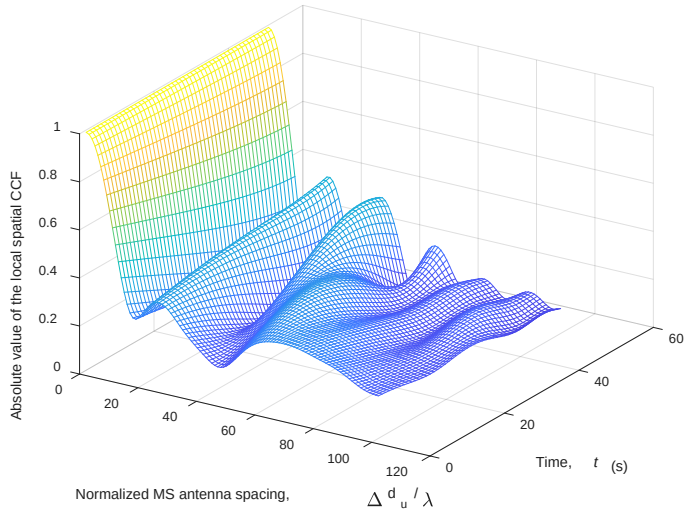

Figure 5: The plot for the absolute value of the local spatial CCF of the non-stationary IMT-A massive MIMO channel model for the open space scenario

The LoS propagation condition for the open space scenario, having the key simulation parameters as follows; $\phi_{n,m}(t_o)$ = random, $D_{BS}(t_o)$ = 100m, $\theta_A = 15^0$, v_A = 30m/s, $\varphi_{n,m}(t_o)$ = random, $D_{MS}(t_o)$ = 150m, $\theta_v = 120^0$, and v = 20m/s (Ghazal, 2017). Figure 5 shows the absolute values of the 3D local spatial CCF of the non-stationary IMT-A massive MIMO channel model, the figure clearly shows that the local spatial CCF changes with time as a result of the non-stationarity of the channel.

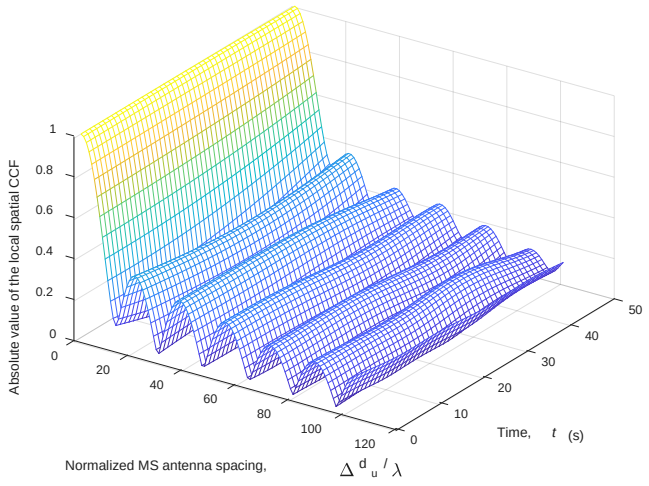

Figure 6: The plot for the absolute value of the local spatial CCF of the non-stationary IMT-A massive MIMO channel model for the viaduct scenario

By adopting the LoS propagation condition for the viaduct scenario, the key simulation parameters used are as follows; $\phi_{n,m}(t_o)$ = random, $D_{BS}(t_o)$ = 100m, $\theta_A = 15^0$, v_A = 30m/s, $\varphi_{n,m}(t_o)$ = random, $D_{MS}(t_o)$ = 150m, $\theta_v = 120^0$, and v = 20m/s (Ghazal, 2017). Figure 6 above shows the absolute values of the 3D local spatial CCF of the non-stationary IMT-A massive MIMO channel model, the figure clearly shows that the local spatial CCF changes quickly with time as a result of the non-stationarity of the channel.

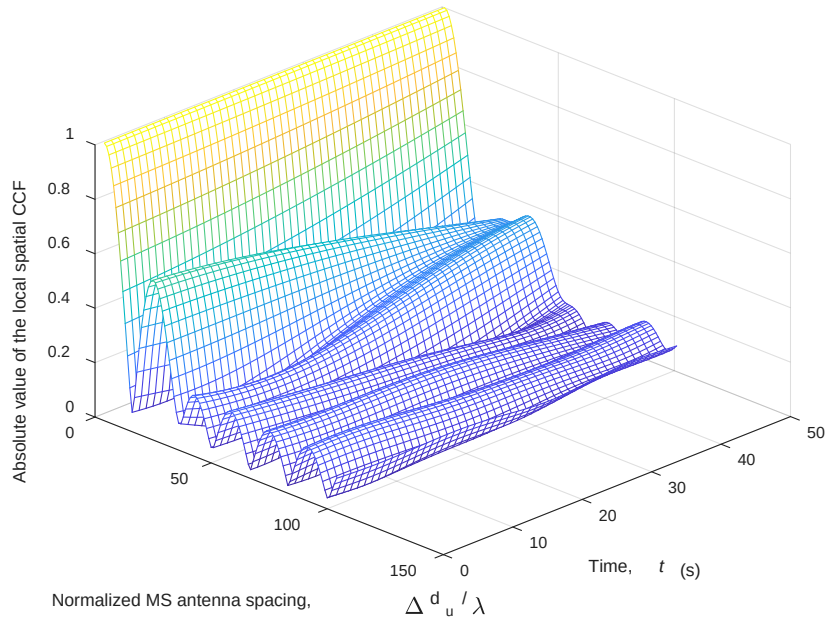

Figure 7: The plot for the absolute value of the local spatial CCF of the non-stationary IMT-A massive MIMO channel model for the cutting scenario

By adopting the LoS propagation condition for the cutting scenario, the key simulation parameters used are as follows; $\phi_{n,m}(t_o)$ = random, $D_{BS}(t_o)$ = 100m, $\theta_A = 15^0$, v_A = 30m/s, $\varphi_{n,m}(t_o)$ = random, $D_{MS}(t_o)$ = 150m, $\theta_v = 120^0$, and v = 20m/s (Ghazal, 2017). Figure 7 above shows the absolute values of the 3D local spatial CCF of the non-stationary IMT-A massive MIMO channel model, the figure clearly shows that the local spatial CCF also changes with time as a result of the non-stationarity of the channel.

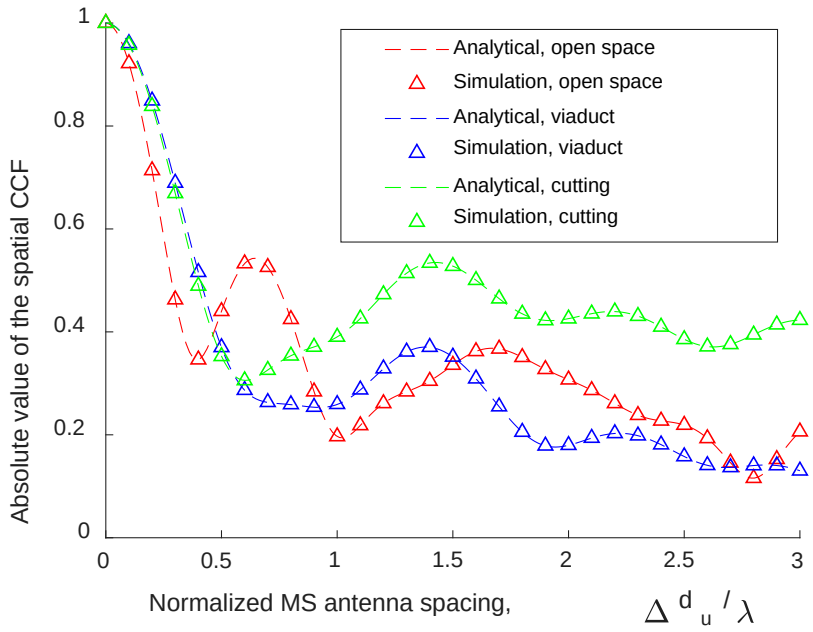

Figure 8: The plot to show the comparison of the local spatial CCFs of non-stationary IMT-A massive MIMO channel model for LoS propagation condition in open space, viaduct and the cutting scenario at *t* = 5s

Figure 8 shows the comparison between the 2D local spatial CCF for open space, viaduct and cutting scenario.

In the cutting scenario, the correlation is very high. This is as a result that the propagation of the radio waveforms is greatly affected by the steep walls and the vegetation on both side due to the U – shaped cut surface between the hills (Wang *et al.*, 2016), which will lead to reflection in the radio waves and more scattered components which leads to more correlation and hence, less channel capacity (Wang *et al.*, 2016; Ghazal *et al.*, 2016; Alshammari *et al.*, 2017; Fu, 2016).

In the open space scenario, the correlation is less than that of the cutting and higher than that of the viaduct scenario. This might be due to the NLoS propagation condition which is common

in this scenario due to sparse scatterers such as buildings, vehicles that are noticed at the receiver side (Wang *et al.*, 2016), this scatterers may lead to diffraction in the signal which leads to more correlation between the antennas and hence, leads to less channel capacity (Alshammari *et al.*, 2017; Fu, 2016).

In the viaduct scenario, the correlation is very low; it is lower than that of the cutting and open space scenarios. This is based on the height of the BS which gives a clear LoS that reduces the impact of the scattering (such as buildings, trees), reflection and diffraction (Wang *et al.*, 2016) on the signal at the receiver and this, in turn, leads to less correlation between the antennas and hence, high channel capacity (Alshammari *et al.*, 2017; Fu, 2016).

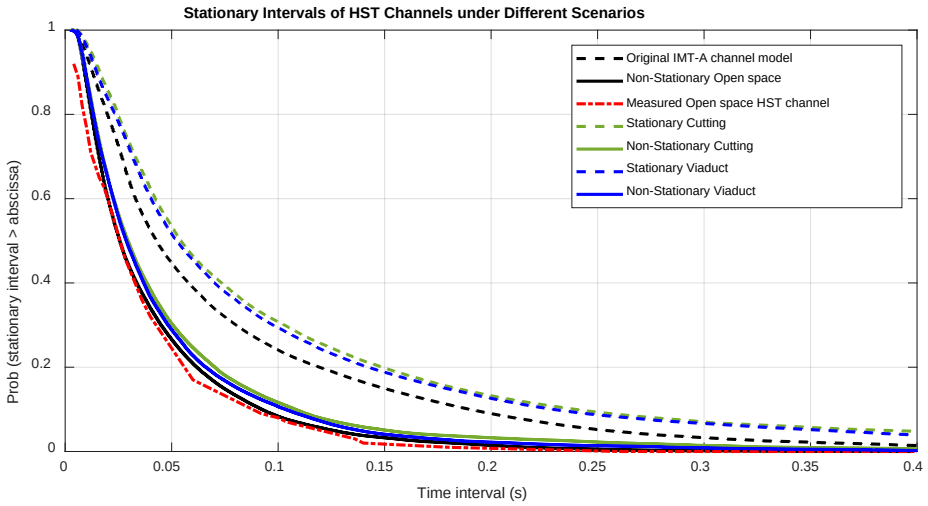

Figure 9: Stationary intervals of HST channels under different scenarios

Figure 9 above shows the plots for the stationary intervals of HST channel under different scenarios. The plots show the empirical complementary cumulative distribution functions (CCDFs) of the stationary intervals for the original IMT-A channel model, proposed non – stationary IMT-A channel model for open space, viaduct and cutting scenarios, and the measured open space HST channel model. The parameters that were used for the simulation are listed as follows: f_c = 930MHz, v = 90m/s and c_{thresh} = 0.8. The parameters for the non-stationary IMT-A channel model is; $D_{BS}(t_O)$ = 100m, v_A = 0m/s, $D_{MS}(t_O)$ = 70m, and θ_v = 0º. (Ghazal, 2017).

Note that the stationary interval in the proposed non-stationary IMT-A massive MIMO channel model depends on the movement parameters such as; the direction of the MC, direction of the MS, AoA spread, AoD spread and so on (Ghazal, 2017).

From Figure 9, it is seen that the proposed channel model agrees well with the measured channel model which demonstrates the feasibility of the proposed non-stationary IMT-A channel models under different HST scenarios. It can also be observed that the stationary intervals for the proposed IMT-A channel model under different HST scenarios and the measured HST open space channel model are considerably shorter than that of the original IMT-A channel model (Ghazal, 2017). A longer stationary interval is observed in cutting than the viaduct and the open space scenario; it might be due to the effect of the reflected and scattered components that are caused by the slopes of the cutting which affects the propagation condition (Wang *et al.,* 2016; Ghazal *et al.,* 2016). The changing in the surrounding environment due to the homogeneous nature of the steep walls of the cutting will affect the communication channel which will make it experience less changes in its propagated path between the transmitter and the receiver compared with the open space and the viaduct scenario.

5.0 Conclusion and Recommendations

5.1 Conclusion

A non-stationary IMT-A massive MIMO channel model has been proposed where the time variation, the channel capacity and the impact of correlation due to the large antenna array in massive MIMO was investigated under different HST propagation scenarios such as; the open space, viaduct and the cutting.

Based on the proposed non-stationary IMT-A, massive MIMO channel model statistical properties such as the local spatial CCF and the local temporal ACF was investigated. The simulation results show that the statistical properties vary with time as a result of the time-varying parameters of the proposed non-stationary channel model. The analytical results were compared with the simulation results, and it was observed that there is good agreement between the analytical and the simulation results which verifies the correctness of the analytical and the simulation result and also demonstrates the correctness of the proposed channel model.

The stationary interval of the proposed channel model under the open space, viaduct and the cutting scenario was also investigated regarding the APDP. The corresponding simulation results prove that the stationary interval of the proposed non-stationary IMT-A massive MIMO channel model match well with the stationary interval of the measured channel model, and it is significantly shorter than the stationary interval of the original IMT-A channel model which

demonstrates that the proposed channel model can mimic the characteristics of the high – mobility channels. From the results, it was also observed that the viaduct and the cutting has a longer stationary interval as compared to the open space.

5.2 Recommendations

The deployment of massive MIMO was to improve the channel capacity in other for the passengers on the train to have more data throughput, but the deployment of this large antenna array at the transmitter and the receiver has an impact on the channel capacity. The impact of the deployment of large antenna on the channel capacity should be thoroughly investigated under different HST propagation scenario. Also, more HST train propagation scenarios such as the tunnel, hilly terrain and the station should be considered in the non-stationary IMT-A massive MIMO channel models.

It is recommended that a non-stationary IMT-A massive MIMO channel model that will verify and investigate the small scale parameters such as; the cluster power, AoDs and AoAs should be considered.

REFERENCES

Ai, B. (2014). Challenges towards wireless communication for high – speed railway. *IEEE Transactions on Intelligent Transportation Systems*, 15(5), 2143 – 2155.

Alshammari, A., Albdran, S. & Matin, M. A. (2017). Optimal Capacity and Energy Efficiency of Massive MIMO Systems. *Intenational Journal of Computer Science Information Security*, 15(6), 13-37.

Bai, L., Wang, C. X., Wu, S., Sun, J. & Zhang, W. (2017). A 3-D Wideband Multi-Confocal Ellipsoid Model for Wireless Massive MIMO Communication Channels with Uniform Planar Antenna Array. *IEEE Vehicular Technology Conference*, June, 2017.

Cheng, X., Yu, B., Yang, L., Zhang, J., Liu, G., Wu, Y. & Wan, L. (2014). Communicating in the real world: 3D MIMO. *IEEE Wireless Communications*, 21(1), 136 – 144.

Fu, Y. (2016). Performance Investigation of Spatial Modulation Systems under Non-Stationary Wideband High-Speed Train Channel Models. *IEEE Transaction on Wireless Communications*, 15(9), 6163–6174.

Gao, X., Tufvesson, F. & Edfors, O. (2013). Massive MIMO channels - Measurements and models. *Asilomar Conference on Signals, Systems, and Computers*, 1(1), 280–284.

Ghazal, A. C. X., Wang, Y., Liu, P., Fan, I. & Chahine, M. K. (2016). A generic non-stationary MIMO channel model for different high-speed train scenarios. *2015 IEEE/CIC International Conference on Communication China, ICCC 2015*.

Ghazal, A. (2017). A non-stationary IMT-advanced MIMO channel model for high-mobility wireless communication systems. *IEEE Transactions on Wireless Communications*, 16(4), 2057–2068.

Guo, Y., Zhang, C. & Tian, L. (2013). Correlation Analysis of High-speed Railway Channel Parameters Based on Channel Measurement. *High Mobile Wireless Communication, (2013) International Workshop*, p. 132 – 136, April, 2013.

Hentilä, L., Kyösti, P., Käske, M., Narandzic, M. & Alatossava, M. (2007). MATLAB implementation of the WINNER Phase II Channel Model ver1.1. Retrieved from: http://projects.celtic-initiative.org/winner+/phase_2_model.html.

Jianhua, Z. (2017). A survey of massive MIMO channel measurements and models," *ZTE Communications*, 15(1), 14 – 21.

Larsson, E., Edfors, O., Tufvesson, F. & Marzetta, T. (2014). Massive MIMO for next generation wireless systems. *IEEE Communications Magazine*, 52(2), 186–195.

Report ITU-R M.2135-1 (2009). Guidelines for evaluation of radio interface technologies for IMT-Advanced. *Evaluation*, 93(3), 22-34.

Sun, R., Tao, C., Liu, L. & Tan, Z. (2013). Channel measurement and characterization for HSR U-shape groove scenarios at 2.35 GHz. *IEEE Vehicular Technology Conference*, 1(1), 1 – 6.

Tian, L., Zhang, J. & Pan, C. (2013). Small scale fading characteristics of wideband radio channel in the U-shape cutting of high-speed railway. *IEEE Vehicular Technology Conference*, 1(1), 1 – 6.

Wang, C. X., Ghazal, A., Ai, B., Liu, Y. & Fan, P. (2016). Channel Measurements and Models for High-Speed Train Communication Systems: A Survey. *IEEE Communications Surveying Tutorials*, 18(2), 974–987.

Wang, C. X., Wu, S., Bai, L., You, X., Wang, J. & Chih, L. I. (2016). Recent advances and future challenges for massive MIMO channel measurements and models. *Science China Information Sciences*, 59(2), 1–16.

Wu, S., Wang, C. X., Aggoune, E. H. M., Alwakeel, M. M. & He, Y. (2014). A non-stationary 3-D wideband twin-cluster model for 5G massive MIMO channels. *IEEE Journal on Selected Areas in Communications*, 32(6), 1207–1218.

Wu, S., Wang, C. X., Aggoune, E. H. M., Alwakeel, M. M. & Ai, B. (2015). A non-stationary wideband channel model for massive MIMO communication systems. *IEEE Transactions on Wireless Communications*, 14(3), 1434–1446.

Wu, S., Wang, C. X., Aggoune, H. M., Alwakeel, M. M. & You, X. H. (2017). A General 3D Non-Stationary 5G Wireless Channel Model. *IEEE Transaction on. Communications*, 20(20), 1–14.

Xie, Y., Li, B., Zuo, X., Yang, M. & Yan, Z. (2015). A 3D geometry-based stochastic model for 5G massive MIMO channels. *Proceedings of 11th EAI International Conference on Heterogeneous Networking for Quality, Reliability, Security and Robustness, QSHINE* 1(1), 216 – 222.

Zhang, P., Chen, J. & Tang, T. (2017). An overview of non – stationary property for massive MIMO channel modelling. *ZTE Communications*, 15(1), 3 – 7.